## General Disclaimer

## One or more of the Following Statements may affect this Document

- This document has been reproduced from the best copy furnished by the organizational source. It is being released in the interest of making available as much information as possible.

- This document may contain data, which exceeds the sheet parameters. It was furnished in this condition by the organizational source and is the best copy available.

- This document may contain tone-on-tone or color graphs, charts and/or pictures, which have been reproduced in black and white.

- This document is paginated as submitted by the original source.

- Portions of this document are not fully legible due to the historical nature of some of the material. However, it is the best reproduction available from the original submission.

75-TR-14

# INVESTIGATIONS OF A BEARING FAULT DETECTOR FOR RAILROAD BEARINGS



By

Donald S. Wilson

John L. Frarey

Shaker Research Corporation
Northway 10 Executive Park
Ballston Lake, N.Y. 12019



Prepared Under Contract No. NAS8-31449

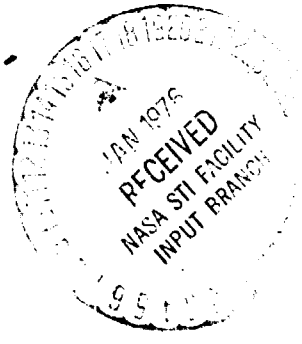


For

NASA-George C. Marshall Space Flight Center

# TABLE OF CONTENTS

## LIST OF ILLUSTRATIONS

## LIST OF TABLES

## INTRODUCTION

As a result of a NASA-supported program conducted in 1971 (References 1 and 2), a technique was developed to detect faults in rolling-element bearings. The technique basically recognizes that damage existing in the raceways or cage areas induces structure-borne vibration in the high-frequency range (10 KHz to 50 KHz) as well as in the low-frequency range (2 Hz to 1000 Hz). Damage is more readily discerned in the high-frequency range and it is possible to identify the damage source by studying the amplitude time history of the high-frequency vibration. Although the technique was originally investigated for use in evaluating ball bearing defects in a control moment gyro, the approach appeared suitable for detection of faults in railroad wheel tapered roller bearings.

In order to verify the suitability of high-frequency vibration as a diagnostic tool for damage in tapered roller railroad wheel bearings, the present program was initiated. This report describes the laboratory tests conducted on new and damaged bearings to determine the feasibility of using high-frequency vibration as a diagnostic tool. A high-frequency band pass filter and demodulator was assembled to permit field measurements of the high-frequency vibrations. Field tests were conducted at the Association of American Railroads facility in Chicago on an actual truck and on an axle assembly run in a grease test rig. These field tests were directed toward demonstration of the suitability and capabilities of the high-frequency technique for field application.

Two specific areas of field application have been identified as being cost effective for railroad use. One area is the examination of railroad roller bearings at a derailment site and the second is as a wayside detector to supplement present hot box detectors for defective roller bearings.

Present Association of American Railroads (AAR) regulations require that each roller bearing that has suffered a derailment must be returned to a bearing rework shop for visual inspection. Cost analysis of this procedure shows that it costs the railroads several hundred million dollars per year

to perform this inspection with the large majority of the bearings found to be in acceptable condition. If this diagnostic technique can perform the inspection at the derailment site without disassembling bearings, it has been calculated that the railroad industry could save $100 million per year.

Present hot box detectors in use by many railroads sense overheated bearings and warn the train crew by some communication system of the dangerous condition. The industry concensus is that this is a valid system to detect defective plain (fluid film) bearings. Roller bearings, however, have several failure modes in which the failure progresses to catastrophic proportions too quickly to be picked up by hot box detectors as presently deployed. The possibility exists that the high-frequency vibration/acoustic technique could provide longer lead time to failure warning than present heat-sensing systems.

ABSTRACT

Fifty eight railroad wheel bearings of the tapered roller type, still in operable condition ranging from new to varying degrees of damage, were evaluated in the laboratory using high-frequency vibrational techniques. A fault detector box was assembled using the high-frequency vibration (10 KHz to 100 KHz) and demodulation techniques for field evaluations. Field tests of selected damaged bearings installed on a railroad truck were conducted using the fault detector to determine the suitability of the technique as a means of detecting bearing damage.

## DISCUSSION

The primary objective of this study was to determine the suitability of high-frequency vibration as a means of detecting damage in railroad wheel roller bearings. In order to accomplish this objective, 58 bearings were obtained ranging from new to badly damaged conditions. The bearings were graded in the laboratory both visually and from vibration levels. Utilizing these results, a fault detection circuit was assembled that was capable of indicating vibration levels in the frequency ranges of interest as determined from test. Several bearings containing different degrees of damage, as determined from laboratory tests, were utilized for field tests assembled on axles. The fault detector box was then used during actual field tests to verify the suitability of the technique under field conditions.

For discussion purposes, the three phases of the study are summarized in the following three subsections:

- Laboratory Tests and Results
- Fault Detector Prototype
- Field Tests and Results

### Laboratory Tests

The test rig used for laboratory evaluation of the railroad bearings is shown in Figure 1. The rig accepts a single tapered roller set in lieu of the double tapered roller found in the complete assembled roller of Figure 2. A cup (Figure 2) is installed in the rig vertically and one cage-roller and cone assembly installed in the upward end of the cup. The cone is loaded axially with a pneumatic load cylinder with a controllable load to 1200 pounds. The cup is driven with a variable-speed drive to equivalent train speeds of 100 mph. Two features of the rig differ from an actual bearing installation--i.e., the axial load maintains all rollers in contact with the cup with equal loading in contrast to the normal radial load encountered in service; the cup is the driven member in contrast to the cone or inner race being driven in normal service. Field tests conducted after completion of rig tests were utilized to verify whether these differences

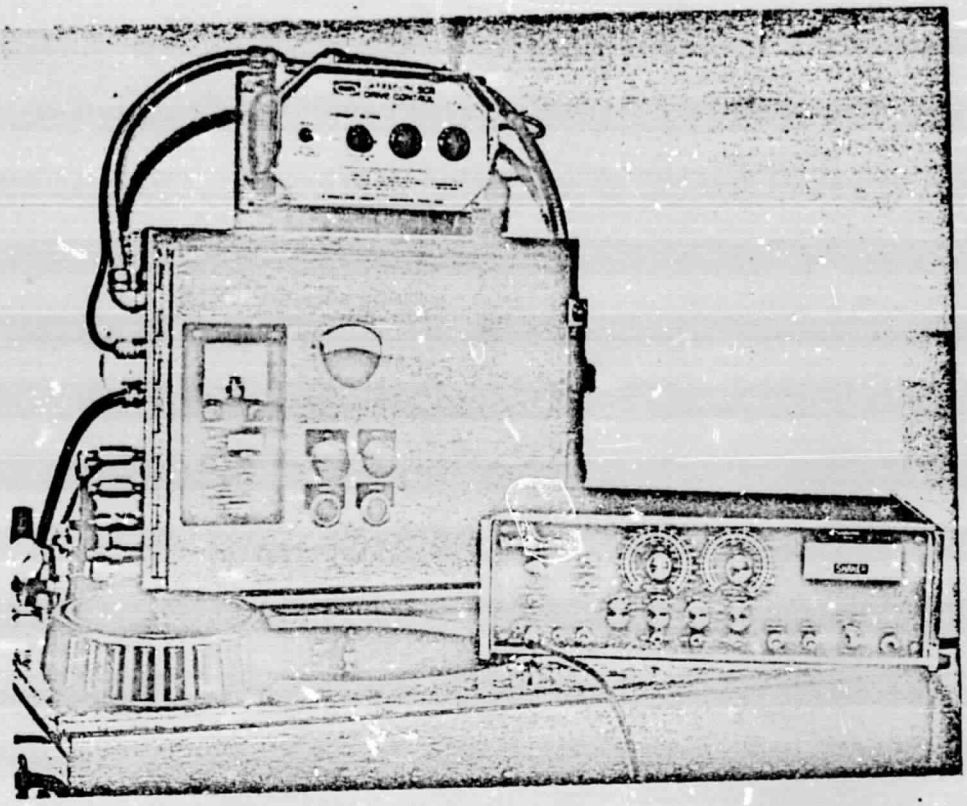

(a) Rig Control Panel and Test Bearing

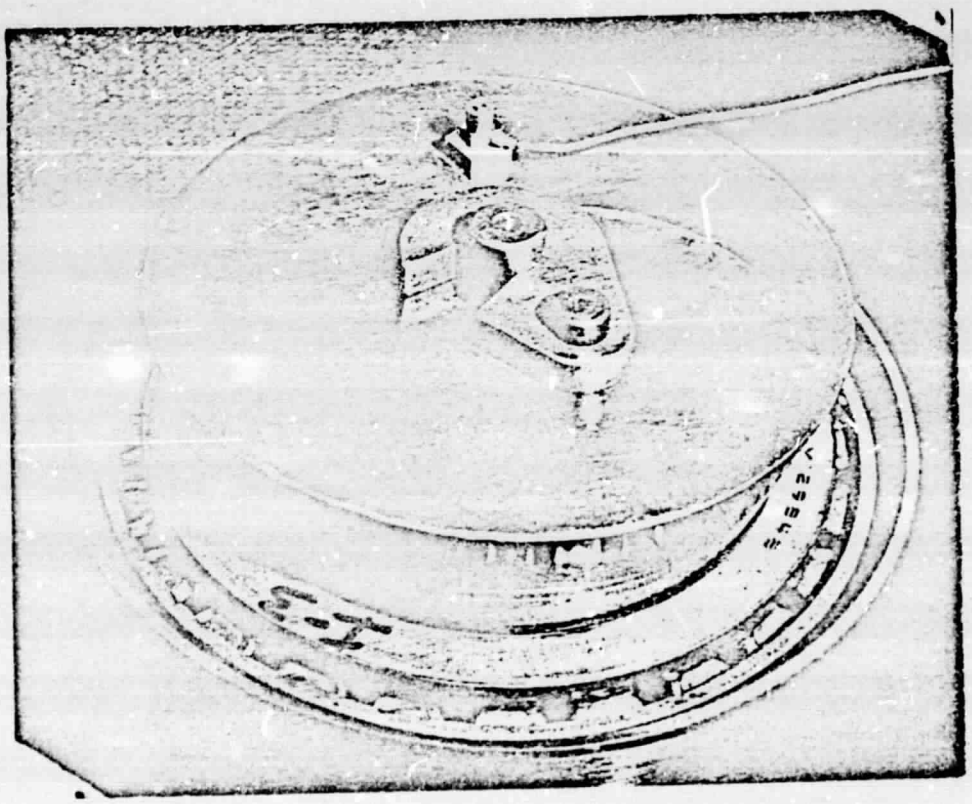

(b) Installed Test Bearing and Accelerometer Pickup



Fig. 1 Bearing Test Rig

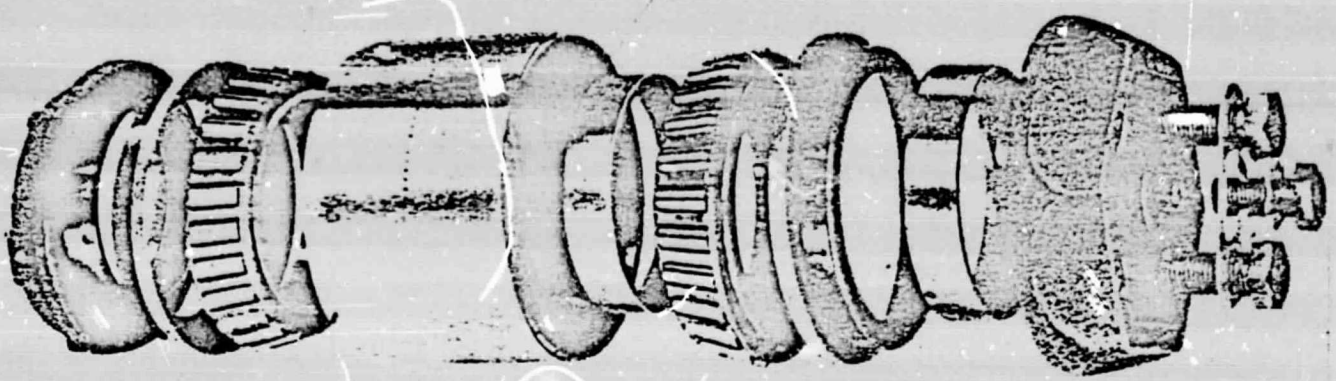

Exploded view of Brenco Crown Taper roller bearing.

**End Cap**—Covers seal and journal end.

**Locking Plate**—Locks cap screws in place.

**Cup**—outer races and external housing.

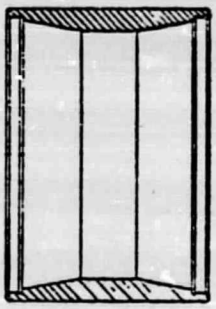

**Cage**—spaces and guides rollers.

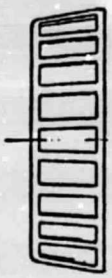

**Roller**—crown-tapered

**Cone**—inner races.

**Spacer**—provides proper lateral spacing of cones.

**Grease Seal**—spring loaded dual lip for positive seal.

**Wear Ring**—provides riding surface for seal.

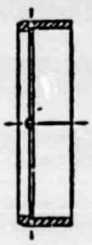

**Backing ring**—provides "backstop" for assembly.



Fig. 2 Journal Boxes: Roller Bearing

had a significant influence on the vibrational characteristics of damaged bearings.

During operation of the rig, the bearing was oil lubricated since the seal and seal ring are not included in the test assembly. Operation was conducted in the 70 to 100 mph equivalent train speed with a 600 pound axial load. A high-frequency response accelerometer was installed on the stationary inner cone to measure bearing vibration to 100 KHz. A 10 KHz high-pass filter was also used to condition the signal--resulting in an analyzing range from 10 KHz to 100 KHz. A high-frequency response microphone (to 70 KHz) was located approximately two feet from the test bearing and also high pass filtered to permit analysis in the 10 KHz to 100 KHz range.

The test procedure consisted of running a number of different roller-cage-cone assemblies ranging from new, used, damaged, and large defects in the same cone. These tests were followed by running a new roller assembly in different degrees of damage cones. The structural and acoustic vibration data were analyzed for frequency content utilizing a real time frequency analyzer. The peak amplitude of sixteen spectra of frequency content versus amplitude of the complex vibration and acoustis data were stored in the computer for further analysis.

## Laboratory Test Results

Fifty three used railroad bearings were obtained for conducting initial evaluations. Twelve contained large visual defects, fifteen were classified as medium level of defect from macroscopic examination, and 26 contained small or undetectable defects. In addition, five unused bearings were also evaluated.

Frequency spectra of three typical bearings are illustrated in Figures 3 and 4. These figures present the peak amplitude level of the complex acceleration and acoustic vibrations as a function of the frequency content during an 0.8 second time period. The results of the acceleration data indicate high levels in the 14 KHz to 20 KHz range and 20 KHz to

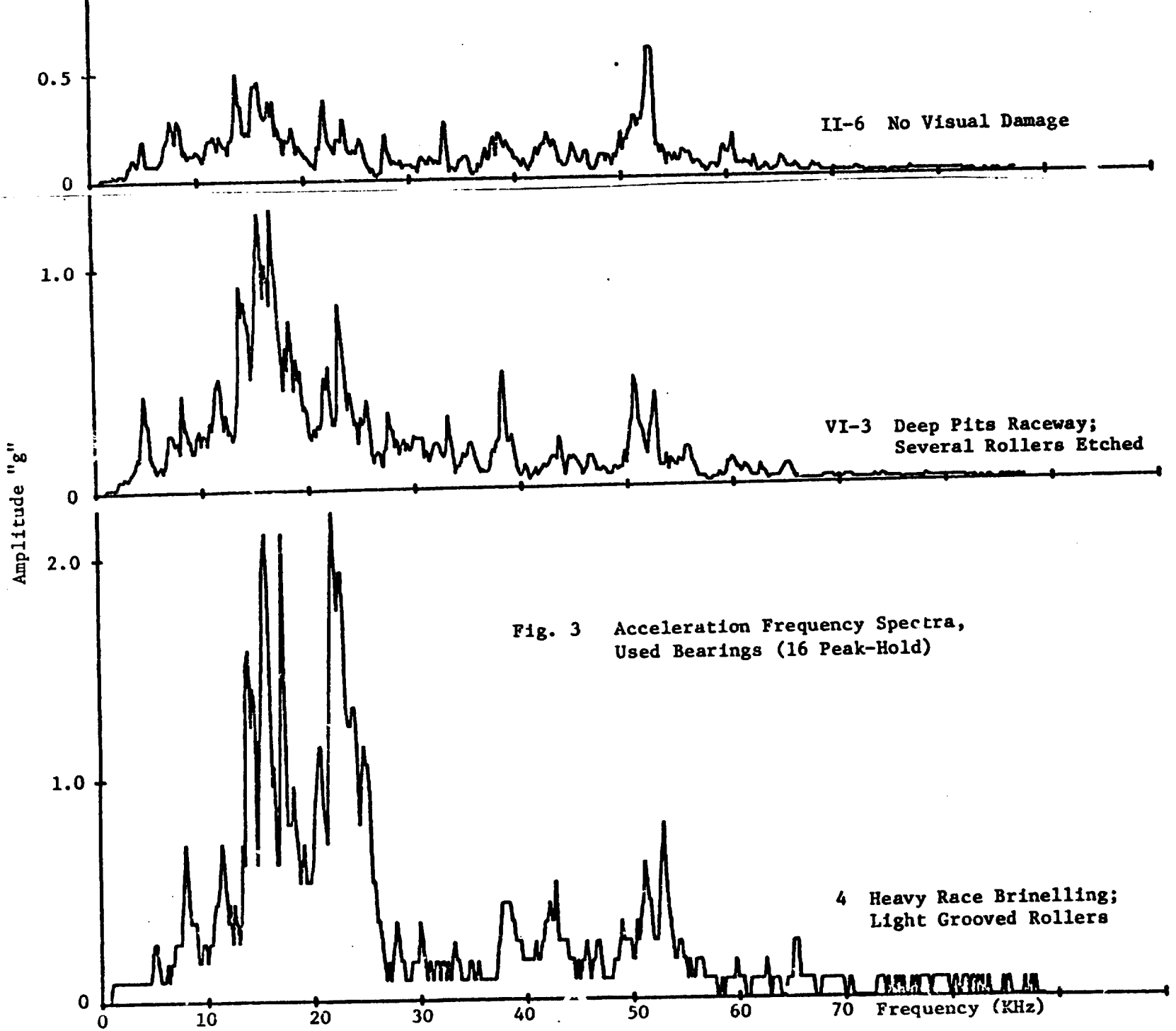


Fig. 3 Acceleration Frequency Spectra,
Used Bearings (16 Peak-Hold)

Fig. 4 Linear Sound Frequency Spectra, Used Bearings (16 Peak-Hold)

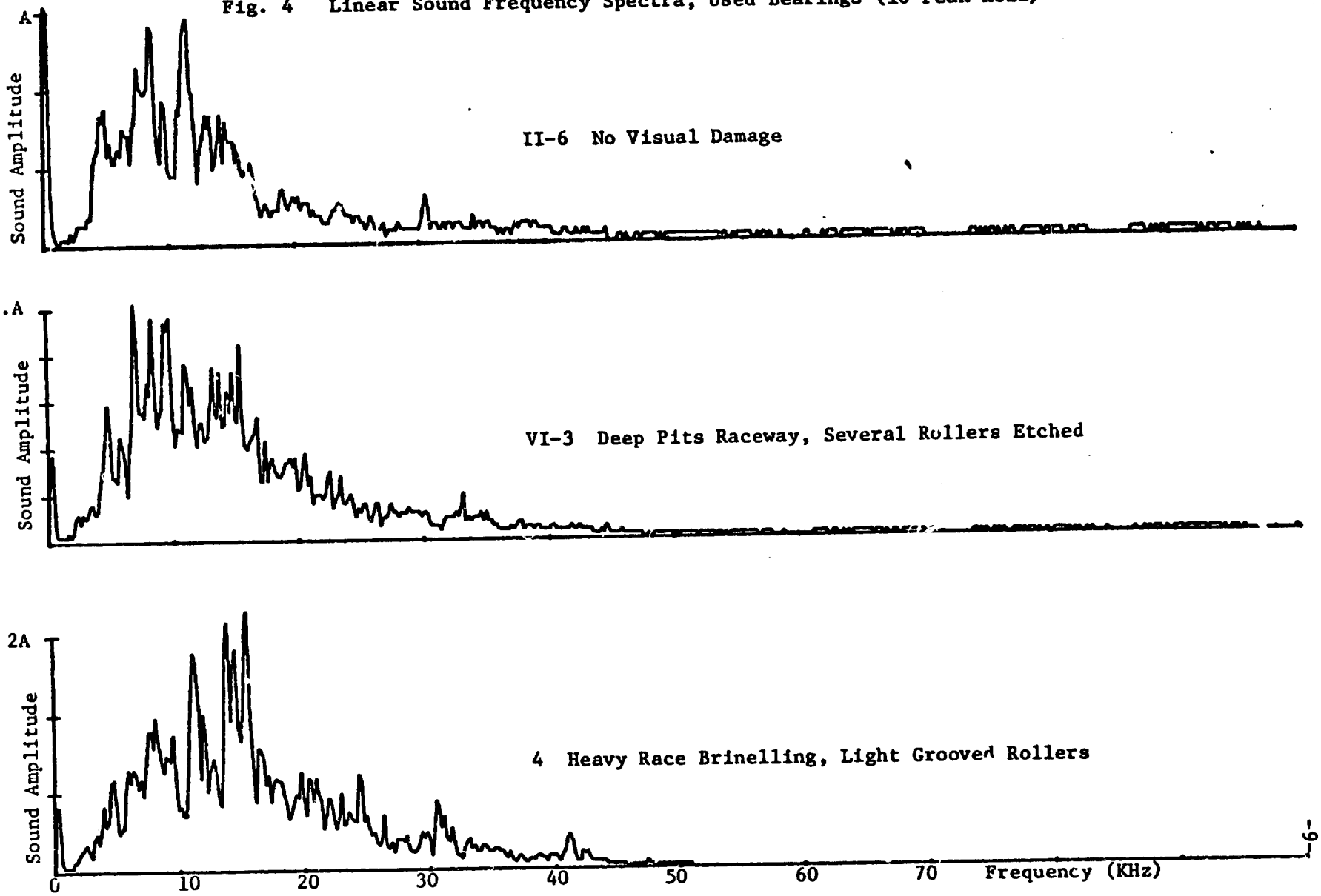

30 KHz range. Measurable increases in levels between an undamaged bearing and damaged bearings is also evident by noting the amplitude scale factor on the figures. In order to rank all bearings relative to amplitude and frequency range, the frequency spectra of the 58 test bearings were searched by computer for the peak amplitude in the following frequency ranges: 14 KHz to 20 KHz; 20 KHz to 29 KHz; and 30 KHz to 40 KHz. Tables 1 and 2 summarize the results of both the sound and vibration frequency data in the three frequency ranges of interest. The trend is evident by inspection of both vibration and acoustic data for higher amplitudes for the large defect bearings. The vibration data provides better resolution between good and bad bearings because of the larger amplitude spread in the results. There was also concern that higher background noise in the field than in the laboratory might seriously influence the sound results. Therefore, additional effort was spent on the vibration data to establish the most suitable frequency analysis range or ranges for fault detection. The distribution of amplitude readings was computed of the large, medium, and small defects for each frequency range. From Figure 5 it is noted that in the 14 KHz to 20 KHz frequency range the distribution is skewed to the left for both the large defects and medium defects while it is a more normal distribution for the small defects. The effect is attributed in part to the discretion used in ranking defects. The visual ranking technique was set up as follows:

Large defect - very evident by eye
Medium defect - evident by close inspection
Small defect - very light or difficult to discern

In the case of medium defects, such things as water etching or bluing are quite evident by eye but were not ranked large since their influence on life was not considered as serious as a defect such as a cracked roller.

From Figure 5, it would appear that two normal distributions could be established with a 1.0 "g" limit used to separate good bearings from bad bearings. This frequency range, therefore, was considered a suitable range for monitoring bearing condition.

Figure 6 is a distribution plot for vibrational amplitudes in the 20 KHz to

TABLE 1

RANKING OF AMPLITUDE LEVELS OF CONE VIBRATION
VERSUS VISUAL CLASSIFICATION OF DEFECT

| Bearing No. | Fault | Defect Class | Peak Amplitude 14K to 20 KHz | 20K to 29 KHz | 30K to 40 KHz |
|---|---|---|---|---|---|
| 5 | Cracked Roller | Large | 9.53 | 10.74 | 3.47 |
| V-5 | Roller High Spot | Large | 19.93 | 9.01 | 10.22 |
| V-2 | Roller High Spot | Large | 3.29 | 1.99 | 1.30 |
| I-3 | Cracked Roller | Large | 12.13 | 5.37 | 4.51 |
| 4 | Brinnell Race | Large | 2.08 | 2.17 | .43 |
| 3 | Brinnell Roller | Large | 3.21 | 2.51 | 1.13 |
| III-2 | Spalled Race | Large | 3.64 | 1.82 | .61 |
| I-4 | Spalled Roller | Large | 1.91 | 1.35 | .90 |
| 87 | Spalled Race | Large | 2.94 | .80 | .64 |
| | Brinnelled Cup | Large | | | |
| 85 | Cracked Cup | Large | 1.75 | .78 | .36 |
| 81 | Broken Cup at Edge | Large | .47 | .35 | .32 |
| III-3 | Pitted Race | Medium | 1.98 | 1.11 | .80 |
| II-5 | Spalled Rollers | Medium | 2.08 | 1.59 | .73 |
| VI-3 | Pitted Rollers | Medium | 1.26 | .83 | .52 |
| V-4 | Spalled Race | Medium | 1.32 | .83 | .42 |
| III-6 | Blued Roller | Medium | .83 | 1.01 | .69 |
| I-5 | Spalled Roller | Medium | 1.20 | .78 | .36 |
| I-6 | Spalled Roller | Medium | 1.37 | .38 | .50 |
| II-2 | Race Gouged | Medium | .94 | .62 | .28 |
| VI-4 | Rust in Race | Medium | .69 | 1.02 | .35 |
| 86 | Spalled Roller & Cup | Medium | 1.39 | .87 | .67 |
| 84 | Water Etch Cup | Medium | 1.04 | .60 | .20 |
| 88 | Water Etch Cup | Medium | .91 | .55 | .61 |
| V-3 | Etched Rollers | Medium | .80 | .76 | .42 |
| VI-2 | Blued Roller | Medium | .83 | .92 | .38 |
| VI-5 | Etched Rollers | Medium | 1.02 | .45 | .19 |

TABLE 1 (Continued)

| Bearing No. | Fault | Defect Class | Peak Amplitude 14K to 20 KHz | 20K to 29 KHz | 30K to 40 KHz |
|---|---|---|---|---|---|
| 13 | No Visable Damage | Small | 1.09 | .88 | .47 |
| I-1 | Light Roller Scuff | Small | .83 | .54 | .31 |
| VI-1 | Light Race Brinnell | Small | 1.16 | .26 | .45 |
| V-6 | Race Scratched | Small | .73 | .87 | .45 |
| 83 | Brinnelled Cup | Small | .36 | .28 | .22 |
| 82 | Spalled Cup | Small | .21 | .19 | .17 |
| 15 | No Visable Damage | Small | .88 | .87 | .54 |
| 9 | Race Spall | Small | .26 | .43 | .35 |
| I-2 | Roller Spall | Small | .66 | .64 | .35 |
| III-4 | No Visable Damage | Small | .68 | .62 | .54 |
| III-1 | No Visable Damage | Small | .59 | .36 | .36 |
| III-5 | Roller Spall | Small | .64 | .50 | .33 |
| 1 | Race Brinnell | Small | .69 | .31 | .35 |
| 2 | Race Spall | Small | .53 | .35 | .36 |
| 6 | Roller Smear | Small | .71 | .40 | .23 |
| 12 | No Visable Damage | Small | .50 | .35 | .24 |
| 16 | No Visable Damage | Small | .59 | .68 | .26 |
| II-3 | Roller Dent | Small | .64 | .36 | .28 |
| VI-6 | Roller Groove | Small | .68 | .26 | .24 |
| II-6 | No Visable Damage | Small | .45 | .36 | .26 |
| II | Race Brinnell | Small | .40 | .29 | .23 |
| 10 | Roller Spall | Small | .40 | .54 | .23 |
| II-1 | Race Spall | Small | .38 | .43 | .23 |
| 14 | No Visable Damage | Small | .52 | .29 | .24 |
| 8 | Roller Grooved | Small | .29 | .30 | .28 |
| 7 | Race Spalled | Small | .33 | .34 | .16 |
| T-1 | None | New | .29 | .28 | .25 |
| T-2 | None | New | .42 | .39 | .23 |
| B-2 | None | New | .47 | .36 | .55 |
| B-1 | None | New | .52 | .50 | .55 |
| B-3 | None | New | .95 | .66 | .47 |

TABLE 2

RANKING OF AMPLITUDE LEVELS OF SOUND
VERSUS VISUAL CLASSIFICATION OF DEFECT

| Bearing No. | Fault | Defect Class | Peak Amplitude 14K to 20 KHz | 20K to 29 KHz | 30K to 40 KHz |
|---|---|---|---|---|---|
| 5 | Cracked Roller | Large | .664 | .719 | 1.014 |
| V-5 | Roller High Spot | Large | .212 | .212 | .101 |
| V-2 | Roller High Spot | Large | .136 | .075 | .049 |
| I-3 | Cracked Roller | Large | .202 | .144 | .075 |
| 4 | Brinell Race | Large | .104 | .081 | .046 |
| 3 | Brinell Roller | Large | .150 | .098 | .133 |
| III-2 | Spalled Race | Large | .139 | .069 | .035 |
| I-4 | Spalled Roller | Large | .121 | .075 | .035 |
| 87 | Spalled Race | Large | - | - | - |
| | Brinelled Cup | Large | - | - | - |
| 85 | Cracked Cup | Large | - | - | - |
| 81 | Broken Cup at Edge | Large | - | - | - |
| III-3 | Pitted Race | Medium | .003 | .003 | .139 |
| II-5 | Spalled Rollers | Medium | .127 | .058 | .058 |
| VI-3 | Pitted Rollers | Medium | .078 | .043 | .029 |
| V-4 | Spalled Race | Medium | .072 | .040 | .026 |
| III-6 | Blued Roller | Medium | .064 | .032 | .029 |
| I-5 | Spalled Roller | Medium | .078 | .075 | .029 |
| I-6 | Spalled Roller | Medium | .069 | .061 | .066 |
| II-2 | Race Gouged | Medium | .064 | .038 | .014 |
| VI-4 | Rust in Race | Medium | .038 | .037 | .022 |
| 86 | Spalled Roller & Cup | Medium | - | - | - |
| 84 | Water Etched Cup | Medium | - | - | - |
| 88 | Water Etched Cup | Medium | - | - | - |
| V-3 | Etched Rollers | Medium | .052 | .032 | .017 |
| VI-2 | Blued Roller | Medium | .043 | .038 | .014 |
| VI-5 | Etched Rollers | Medium | .058 | .035 | .014 |

TABLE 2 (Continued)

| Bearing No. | Fault | Defect Class | Peak Amplitude 14K to 20 KHz | 20K to 29 KHz | 30K to 40 KHz |
|---|---|---|---|---|---|
| 13 | No Visible Damage | Small | .047 | .045 | .018 |
| I-1 | Light Roller Scuff | Small | .040 | .038 | .017 |
| VI-1 | Light Race Brinell | Small | .040 | .032 | .014 |
| V-6 | Race Scratched | Small | .040 | .027 | .016 |
| 83 | Brinelled Cup | Small | - | - | - |
| 82 | Spalled Cup | Small | - | - | - |
| 15 | No Visible Damage | Small | .069 | .052 | .040 |
| 9 | Race Spall | Small | .044 | .025 | .025 |
| I-2 | Roller Spall | Small | .029 | .026 | .012 |
| III-4 | No Visible Damage | Small | .042 | .028 | .017 |
| III-1 | No Visible Damage | Small | .043 | .023 | .017 |
| III-5 | Roller Spall | Small | .040 | .029 | .017 |
| 1 | Race Brinell | Small | .029 | .017 | .016 |
| 2 | Race Spall | Small | .044 | .020 | .020 |
| 6 | Roller Smear | Small | .049 | .035 | .014 |
| 12 | No Visible Damage | Small | .027 | .017 | .012 |
| 16 | No Visible Damage | Small | .037 | .027 | .014 |
| II-3 | Roller Dent | Small | .025 | .014 | .012 |
| VI-6 | Roller Groove | Small | .040 | .034 | .014 |
| II-6 | No Visible Damage | Small | .035 | .017 | .012 |
| II | Race Brinell | Small | .028 | .016 | .018 |
| 10 | Roller Spall | Small | .035 | .018 | .014 |
| II-1 | Race Spall | Small | .028 | .015 | .008 |
| 14 | No Visible Damage | Small | .077 | .096 | .041 |
| 8 | Roller Grooved | Small | .022 | .013 | .015 |
| 7 | Race Spalled | Small | .030 | .020 | .015 |
| T-1 | None | New | .024 | .018 | .017 |
| T-2 | None | New | .027 | .028 | .016 |
| B-2 | None | New | .035 | .017 | .021 |
| B-1 | None | New | .032 | .029 | .023 |
| B-3 | None | New | - | - | - |

Fig. 5 . Distribution of Vibration Amplitude in 14 KHz to 20 KHz Range

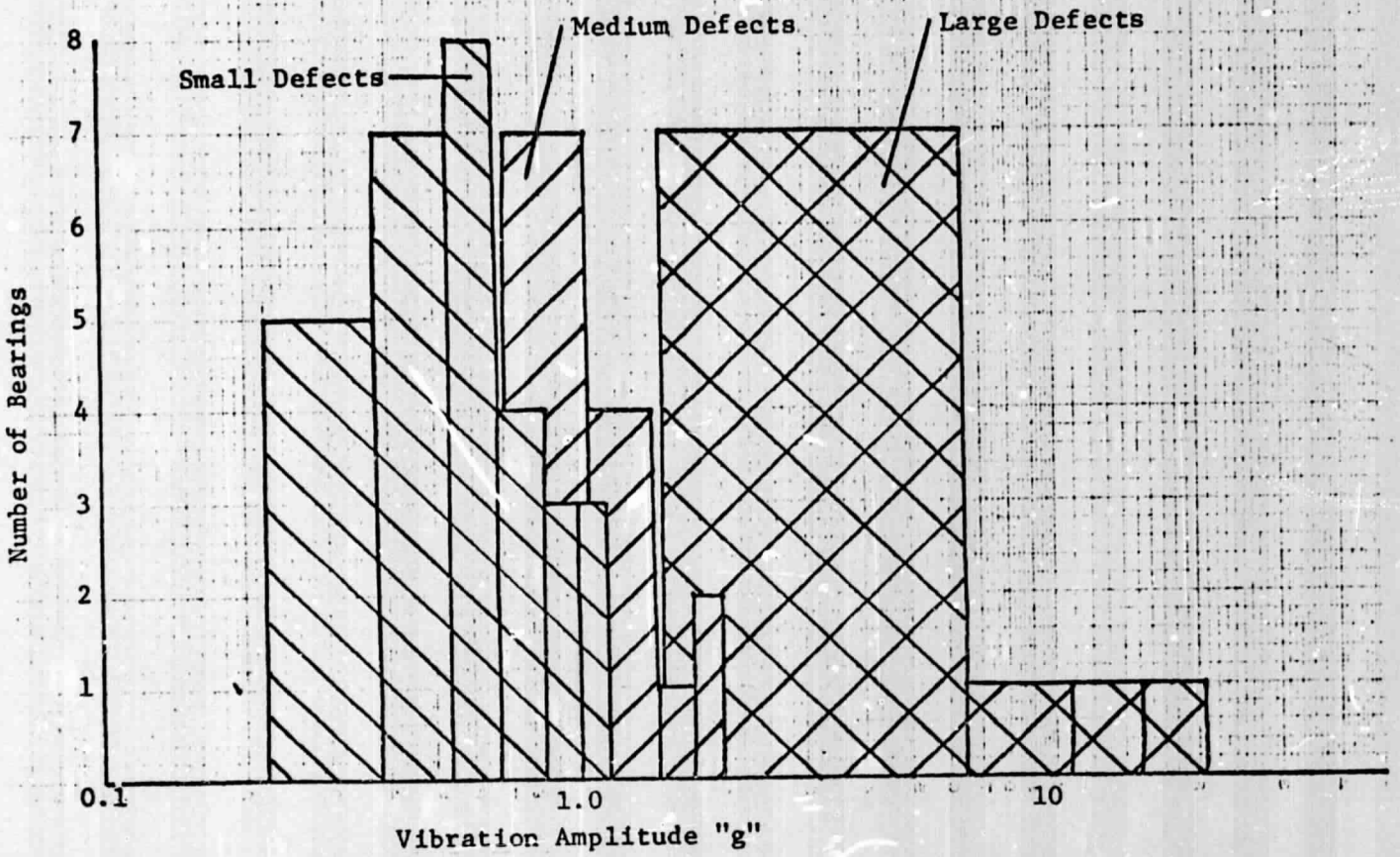

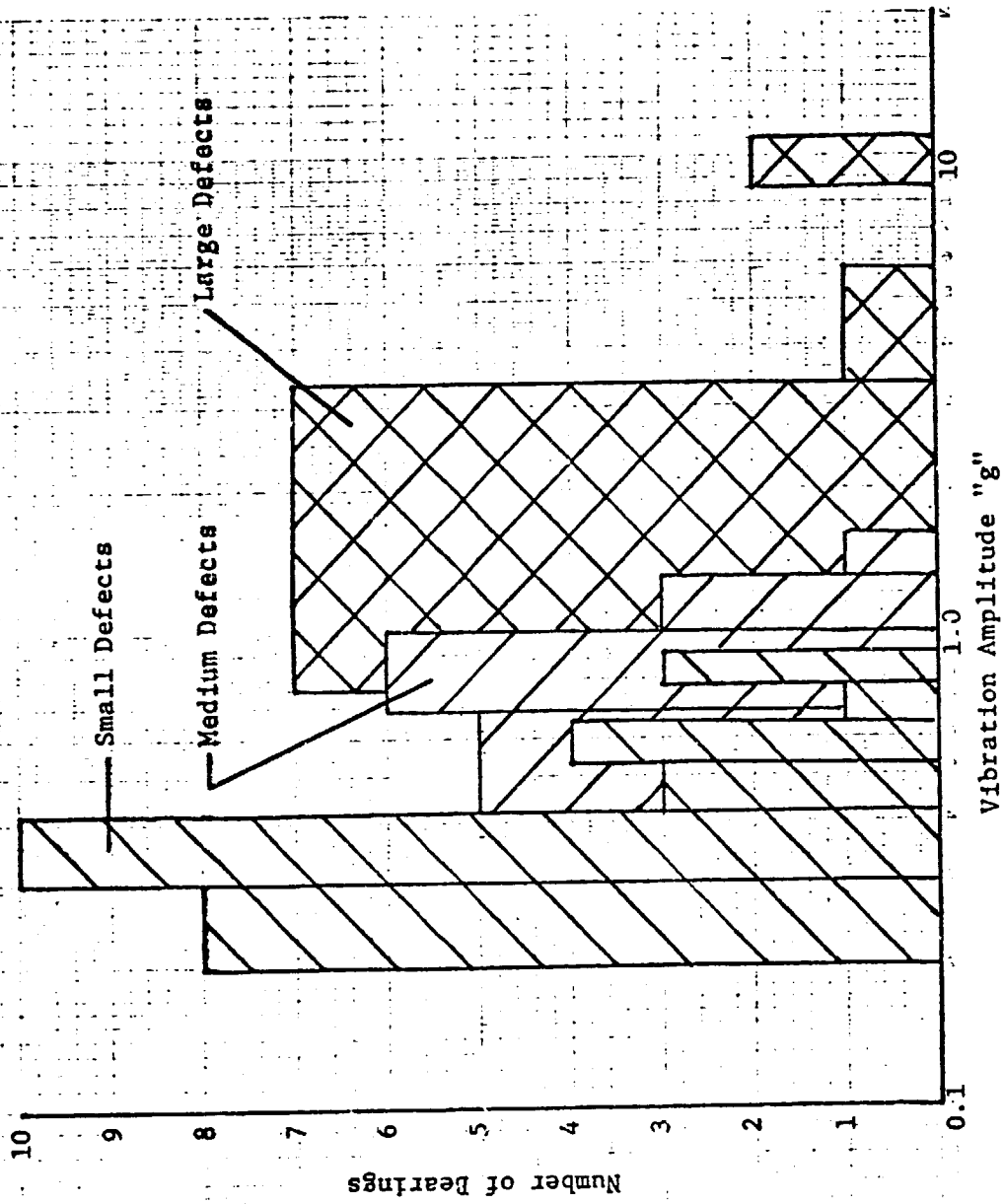


Fig. 6 Distribution of Vibration Amplitude in 20 KHz to 29 KHz Range

29 KHz frequency range. Distributions are quite similar to those in the lower frequency range although the amplitude range is not as large. If an amplitude limit in the range of 0.5 "g" is selected to divide good bearings from bad bearings, a skewed distribution still exists in this frequency range. Although it appears that this range could be utilized, the lower range provides a clearer separation of defects. The distribution for the highest frequency range (30 KHz to 40 KHz) provides the poorest correlation in separating bearings as seen from Figure 7. The medium defects indicate a random distribution as does the small defects making separation of defects difficult. This frequency range was not considered suitable for monitoring.

As a result of these studies, the 14 KHz to 20 KHz range was selected as most suitable for detection of faulty bearings and the 20 KHz to 29 KHz range as an alternate range. In order to further verify the suitability of these ranges, the vibrational outputs of the bearings were subjected to demodulation techniques. Two different frequencies, 16 KHz and 22 KHz, were selected for demodulation since the vibrational amplitudes at these frequencies were time variable. Each frequency was passed through a band pass filter with the center frequency selected at either the 16 K or 22 KHz range. The time variable amplitude was envelope detected and subjected to a frequency vibration analysis. The purpose of this analysis was to determine the driving frequencies that excited the higher frequencies of 16 K and 22 KHz.

Figures 8 and 9 indicate the difference in demodulated characteristics of the 16 KHz and 22 KHz center frequency. At 16 KHz only a low-frequency (7 Hz) driving frequency which is the cage rotational frequency of the bearing. A much stronger signal is noted from demodulation of the 22 KHz center frequency (Figure 9) at the roller pass frequency. Nine bearings were selected for demodulation and the results are tabulated in Table 3. Four bearings with large defects all contain roller pass frequency information at 22 KHz. The bearing with a medium defect (no. VI-3) also contains discrete information of the ball pass frequency. The remaining bearings contained primarily noise with no discrete information at either the 16 KHz

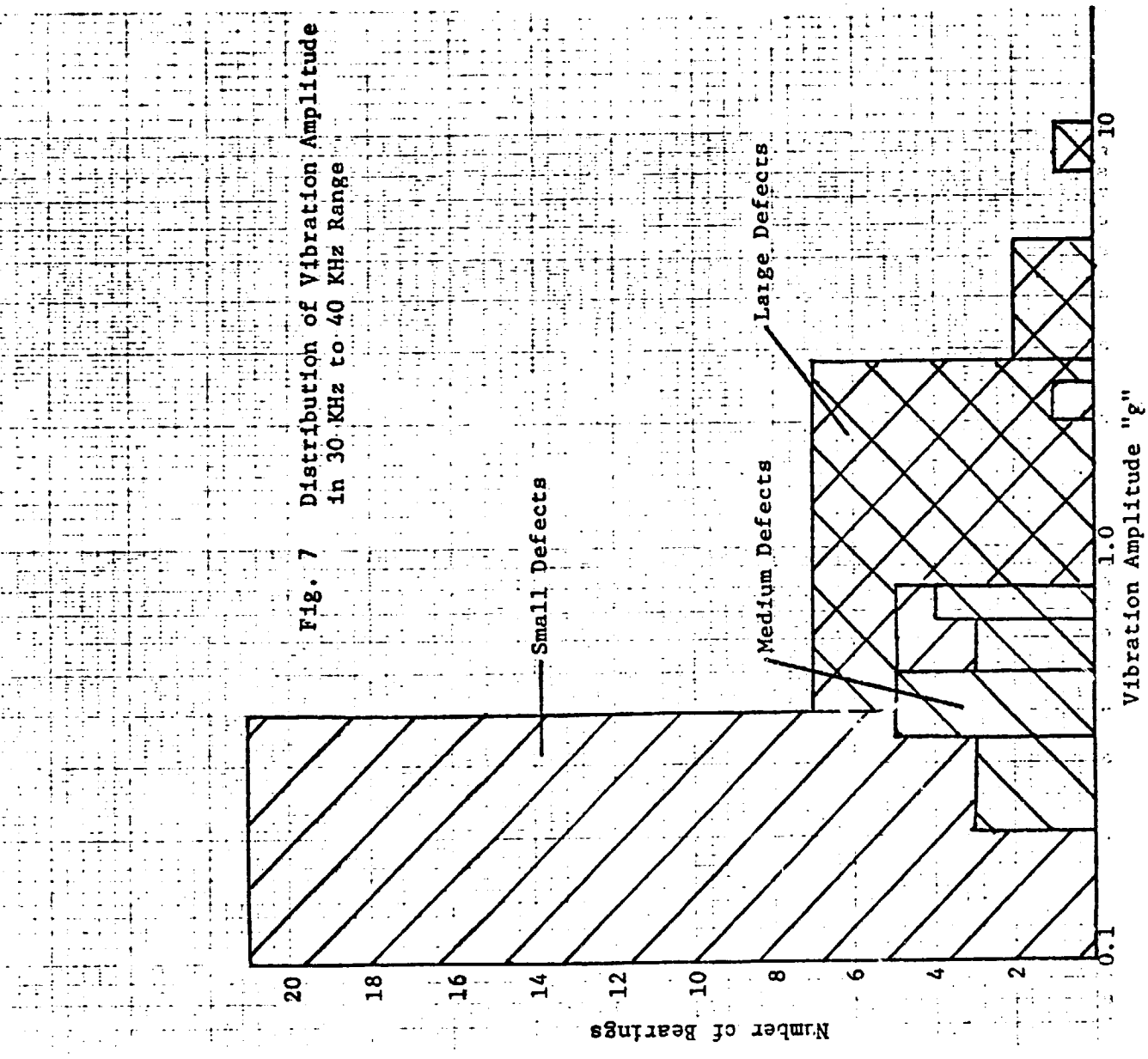


Fig. 7 Distribution of Vibration Amplitude in 30 KHz to 40 KHz Range

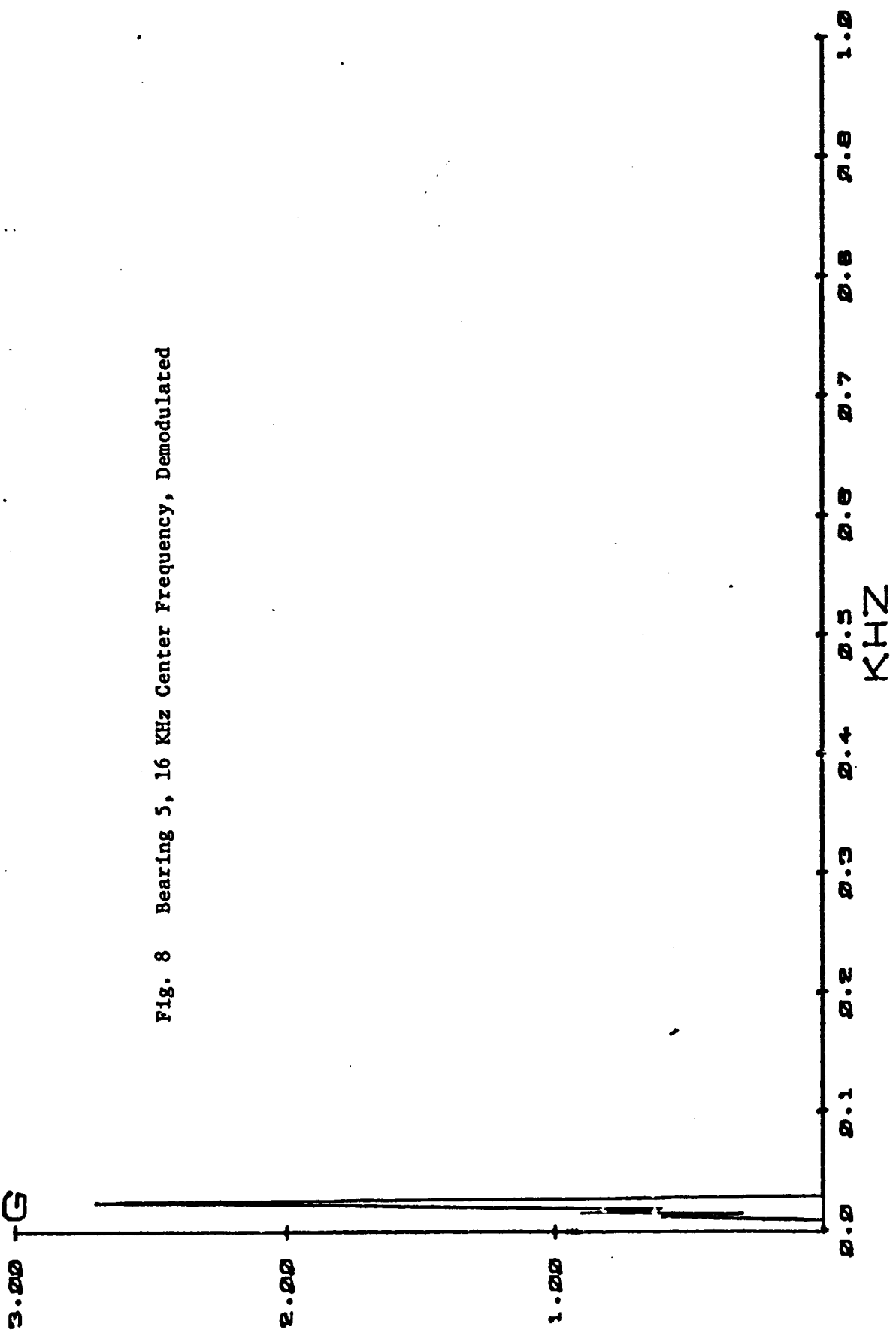


Fig. 8 Bearing 5, 16 KHz Center Frequency, Demodulated

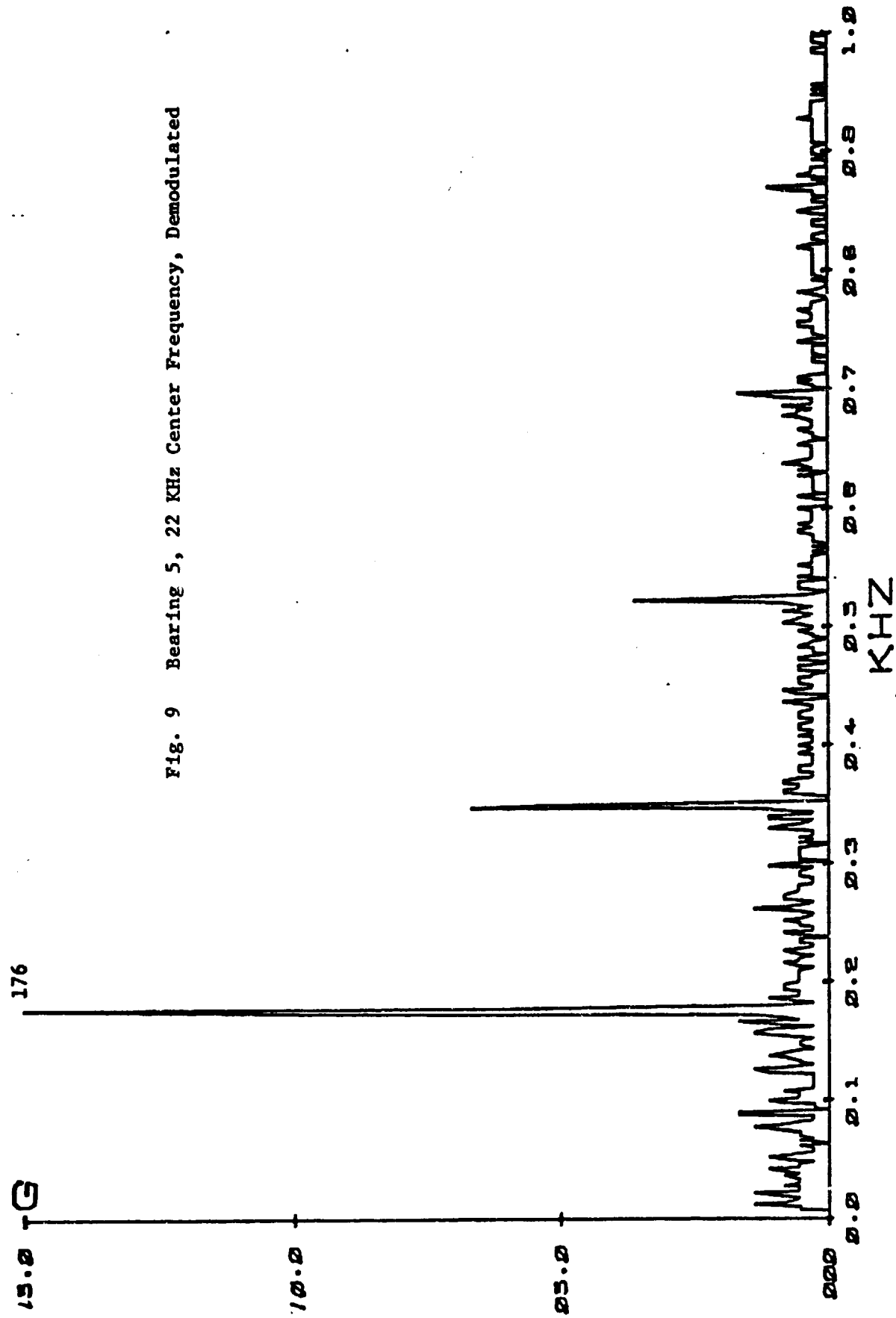


Fig. 9 Bearing 5, 22 KHz Center Frequency, Demodulated

TABLE 3

FREQUENCY SPECTRA OF
DEMODULATED INNER RACE AND ROLLERS

| Defect Class | Bearing No. | 16 KHz Demodulated | 22 KHz Demodulated | Test rpm | Roller Pass rps |
|---|---|---|---|---|---|
| Large | 5 | 2.7 @ 7 Hz | 15 @ 176 Hz | 880 rpm | 176 |
| Large | V-5 | 5.5 @ 172 Hz | 4 @ 172 Hz | 860 rpm | 172 |
| Large | 4 | .0015 @ 202 Hz | 1.4 @ 206 Hz | 1030 rpm | 206 |
| Large | V-2 | 3.5 @ 158 Hz | 1.9 @ 158 Hz | 790 rpm | 158 |
| Medium | VI-3 | .02 @ 7 Hz | .09 @ 208 Hz | 1040 rpm | 208 |
| Small | 13 | .0665 @ 460 Hz | .077 @ 310 Hz | 930 rpm | 186 |
| Small | 15 | .0586 @ 76 Hz | .039 @ 222 Hz | 1010 rpm | 202 |
| Small | 6 | .0743 @ 84 Hz | .038 @ 20 Hz | 830 rpm | 166 |
| New | 3 | .027 @ 305 Hz | .033 @ 156 Hz | 780 rpm | 156 |

or 22 KHz center frequencies. The results indicate that the higher amplitude levels of the 16 KHz and 22 KHz center frequency are dirven by damaged conditions of the bearings. This tends to verify the suitability of these frequencies as satisfactory monitoring areas for detection of bearing damage.

Fault Detector Prototype

The block diagram for the engineering model fault detector is shown in Figure 10. Four sets of data are shown that characterize the signal at four different points in the circuit and also relate to examples of data processing previously discussed. Three of these sets show both the frequency and time domain signals while the output of band pass filter B is an almost pure tone shown only in the time domain.

The block diagram as shown in Figure 10 is the most versitile. Data obtained to date indicates that possibly not all blocks would be required in the final unit and that some controls and outputs could be eliminated to simplify the operation; however, for the present program, the maximum sensitivity shown was retained. The example of the processed data in Figure 10 is for the switch portion shown. The description of the block diagram follows:

There are two inputs to the unit--one labeled accelerometer input and one voltage input.

When the fault detector is used on a bearing in real time, the accelerometer mounted to the bearing is connected to the charge amplifier which conditions the data (removes effect of cable capacitance) and normalizes it to take into account different accelerometer sensitivities. If magnetic recordings of data obtained during bearing tests are made, this type of data is played back into the volt in input and bypasses the charge amplifier. In the next stage of the unit, a high pass filter may be inserted or bypassed. Because the sound and acceleration data contains high level low-frequency components, the filter was used for the testing to permit the greatest possible dynamic

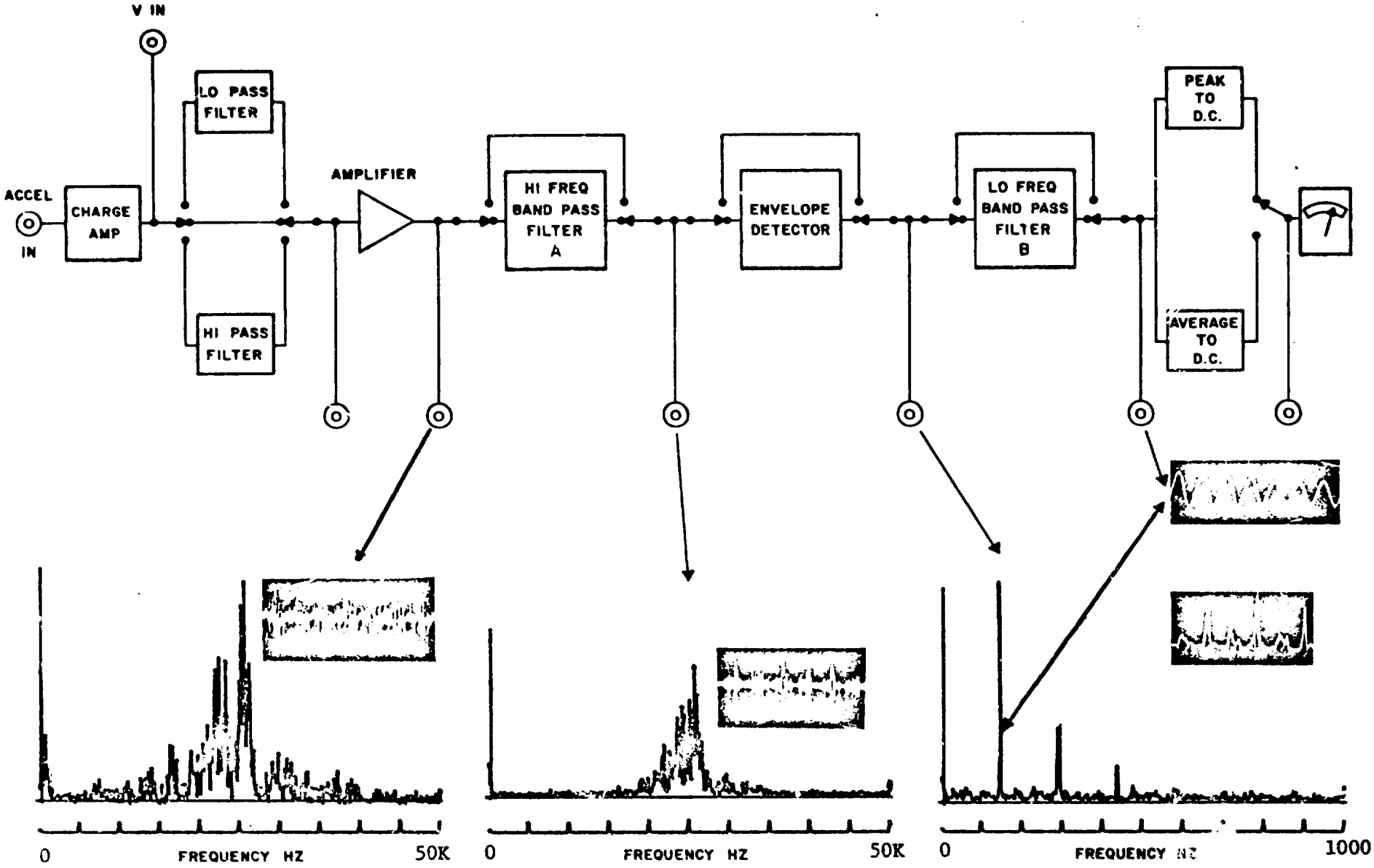


Fig. 10 Fault Detector Box

range of high-frequency data.

Following the high pass filter is a step amplifier to insure adequate signal level for filtering and demodulating. Illustrated on Figure 10 is a frequency spectrum of the high passed data accompanied by a picture of the raw data following the amplifier.

The signal passes from the amplifier to a tunable high pass filter. The filtered data at a center frequency of 22 KHz is illustrated with a frequency spectrum of the frequency content of the filtered wave. The amplitude envelope of the 22 KHz is detected through a demodulator. The envelope and its frequency spectra showing roller pass frequency is also shown in Figure 10. The low pass tunable filter was used to pass the roller pass frequency to check its amplitude.

A selectable peak and average reading meter was used to visually observe the peak amplitudes of the high-frequency band passed data and the demodulated low pass roller frequency.

The fault detector box has two tunable filters which were considered necessary since it was not certain that the same frequencies observed in the laboratory would be encountered in the field. Ultimately a box for field use could contain fixed filters and warning lights to indicate good or bad bearings. This, however, requires verification of the frequencies and amplitude levels as encountered in the field.

## Field Tests

Laboratory tests indicated that vibration in the frequency range of 14 KHz to 20 KHz and 20 KHz to 30 KHz increased in amplitude when bearing damage was encountered. Demodulation of 16 KHz and 22 KHz center frequencies verified that amplitudes in these ranges were time variable and driven by once-per-revolution and roller-pass frequencies. These tests, however, were conducted by instrumenting the inner race and using oil drip lubrication. In order to verify the high-frequency vibration technique in a

fully-assembled bearing, grease packed and installed on a railroad axle, six bearings were selected from the laboratory tests for field testing; i.e.: V-2, 5, V-5, V-4, VI-2, and 85. Since the assembled bearing contains two roller assemblies, the following combinations were assembled:

a) V-2 and 5 assembled with a new cup
   (5 contained a cracked roller)
   (V-2 contained a roller high spot)

b) V-5 and V-4 assembled with a new cup
   (V-5 contained a roller high spot)
   (V-4 contained a medium spalled cone)

c) VI-2 and new roller T-1 with cup 85
   (VI-2 contained blued roller)
   (85 was a cracked cup)

d) B-3 and B-1 with new cup
   (Both B-3 and B-1 were new rollers tested in lab)

e) Two new untested rollers with new cup

The field tests were conducted at the Association of American Railroads in Chicago. Their facilities permitted operation of the bearings assembled on a wheel assembly in a grease test rig as well as assembly of the axle on a truck which was drawn down a test track section.

Three axles were utilized for the experimental program assembled as follows:

Axle 1: End A - Bearings B-3 and B-1 (new bearings previously tested at Shaker Research) with new cups.
End B - New bearings untested previously.

Axle 2: End A - V-5 one roller containing a high spot (classified as a large defect) and V-4.
End B - New bearing untested previously.

Axle 3: Run 1 End A - VI-2 blued roller (classified as medium defect). T-1 new bearing with cup no. 85 (cracked cup large defect).
End B - New bearing untested previously.

Axle 3: End A - V-2 roller high spot (classified as large defect). 5-cracked rollers (classified as large defect).
Run 2

The AAR grease test machine was utilized for evaluation of each axle combination. The machine accepts the test axle supported at the bearing locations and is capable of equivalent train speeds of 60 mph. The test axle was instrumented with an accelerometer pickup on the cup (outer race) of the bearing assembly at each end of the axle. Vibration data and sound were recorded at approximately 60 mph and during coastdown.

Figure 11 is a photograph of the grease test rig illustrating the belt drive and bearing support arrangement. Figure 12 illustrates the location of the accelerometer (O.D. of outer race at 1 o'clock position) and speed pickup (5 o'clock position). Viewing Figures 13 and 14, it may be observed the accelerometer pickup was located axially approximately midway between rollers to permit recording of damage of either roller.

Each axle was instrumented and tested in the grease test machine in the same fashion. Axles 1 and 2 were also installed on a truck utilizing the same instrumentation arrangement and pushed down a test section of track. The instrumentation was carried on the truck during these tests as illustrated in Figure 15. The truck was pushed by hand with forward speeds below 5 mph. Accelerometers were then switched to the underside of the truck and the sound meter placed along the side of the track. The truck was then pushed down the track and data collected during pass by of the truck over the accelerometer location.

Figure 16 illustrates the wheel passing over the location of the accelerometer. Under close examination the accelerometer pickup may be seen

During both the rolling tests and the grease rig tests, peak meter readings were taken from the fault detector box and all data was recorded on magnetic tape for laboratory analysis.

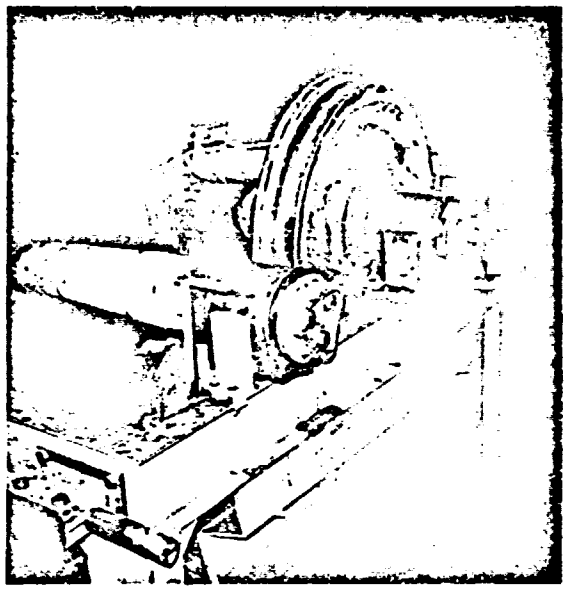

Fig. 11 Railroad Roller Bearing, Grease Test Rig at AAR, Chicago



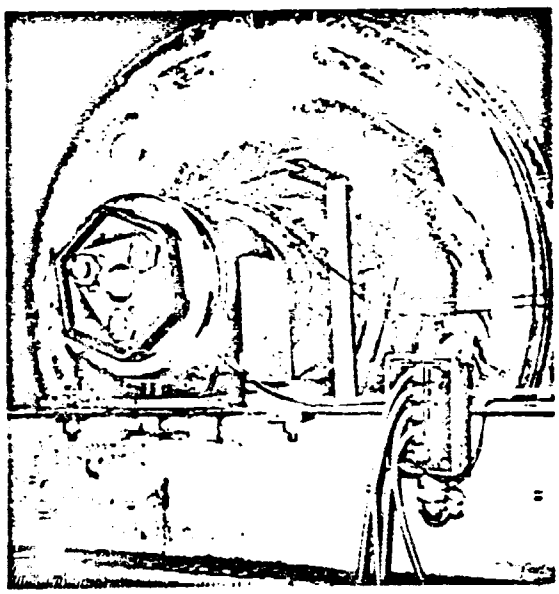

Fig. 12 Instrumented Bearing in Bearing Grease Test Rig

Fig. 13 Bearing-Axle Assembly Schematic

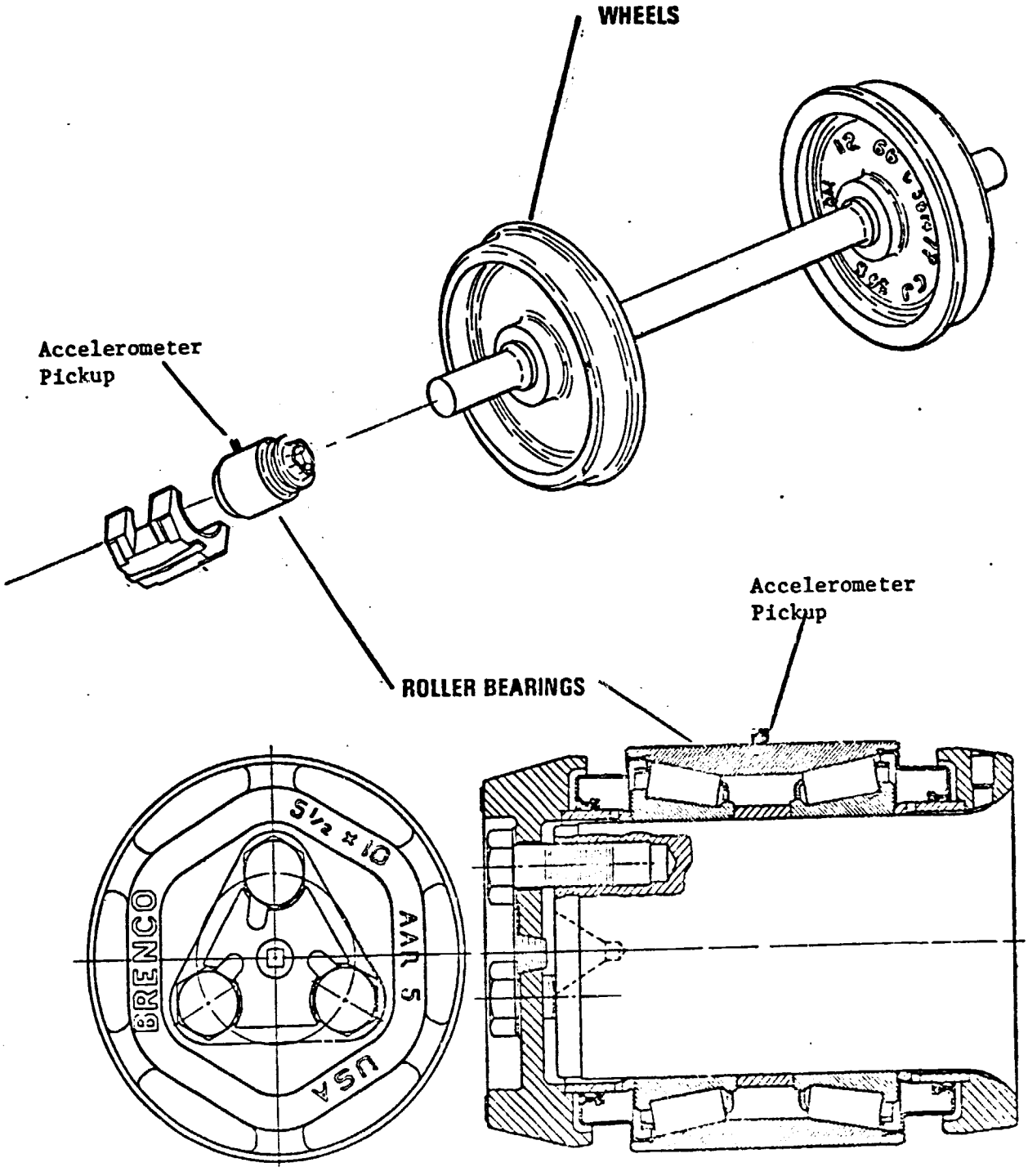


Fig. 14 Bearing Cross Section
(Brenco, Incorporated)

Fig. 15 Instrumented Axles Installed on Truck



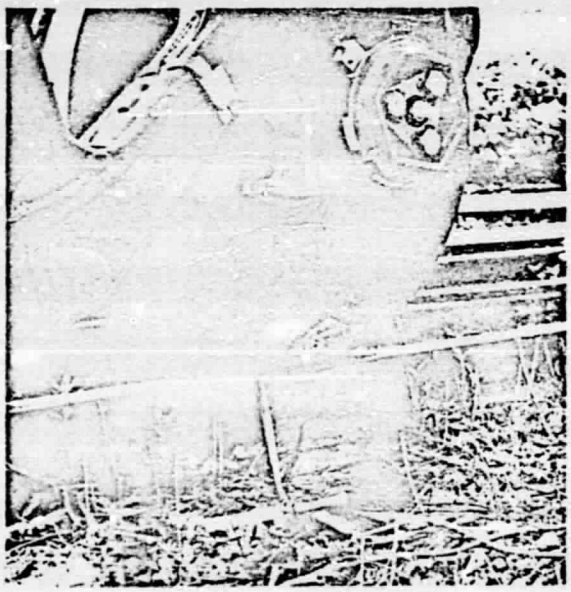

Fig. 16 Track Instrumentation for Roll-By Tests

## Field Test Results

During the grease rig testing, operation was maintained at 610 rpm (± 20 rpm) which approximates a train speed of 60 mph. At this speed, the roller pass frequency is approximately 100 Hz. The fault detector box was used to search the frequency range of 10 KHz to 50 KHz. High amplitudes were noted at 10 KHz and 17 KHz. These frequencies were demodulated and searched in the range of 100 Hz for the presence of roller pass frequency as the driving frequency. High amplitude at roller pass frequency was observed at both frequencies. Table 4 summarizes the meter readings of the acceleration level of both center frequencies. During rolling tests, amplitudes in this range were too low to read and no demodulation components could be discerned.

Tape recorded data was returned to the laboratory for further analysis. Initially, a frequency spectrum versus speed was recorded during coastdown. Figure 17 is frequency spectra plots of bearings V-2 and 5 end of the axle during shutdown. As noted during observations in the field, dominant frequencies at 10 KHz and 17 KHz persist with reasonable amplitude to speeds of approximately 25 mph. At speeds below 5 mph, amplitudes are very low. A similar plot conducted on a new bearing with the same amplitude scale illustrates the obvious differences on Figure 18.

Coastdown data was recorded for each bearing set with a band pass frequency of 10 KHz and 17 KHz. The data was quite similar for both center frequencies.

Figure 19 illustrates the amplitude versus speed characteristic of three sets of damaged bearings and two sets of new bearings. From this plot it can be evidenced that at speeds below 20 mph it is difficult to discriminate between damaged and new bearings as already noted from Figure 17. A jump is evidenced in bearing VI-2, T-1 during coastdown at approximately 54 mph. This bearing contained a cracked cup. It is suspected that the load was sufficient at the higher speeds to open the crack causing higher impact levels then at speeds below 54 mph. The load in the grease test

TABLE 4

FAULT DETECTOR METER READINGS

| Bearing | 10 KHz | 100 Hz Demod. from 10 KHz | 17 KHz | 100 Hz Demod. from 17 KHz |
|---|---|---|---|---|
| B1 & B3 | 7.2 | 2.4 | 6.0 | 2.8 |
| V-5 & V-4 | 80 | 90 | 68 | 88 |
| New & New | 3.4 | 1.4 | 3.0 | 1.2 |
| VI-2 & T-1 With Cup 85 | 28 | 2.5 | 15 | 14 |
| V-2 & 5 | 70 | 80 | 84 | 92 |

Fig. 17 Damaged Bearing; Bearing Frequency Characteristics During Shutdown (Bearing V-2,5)

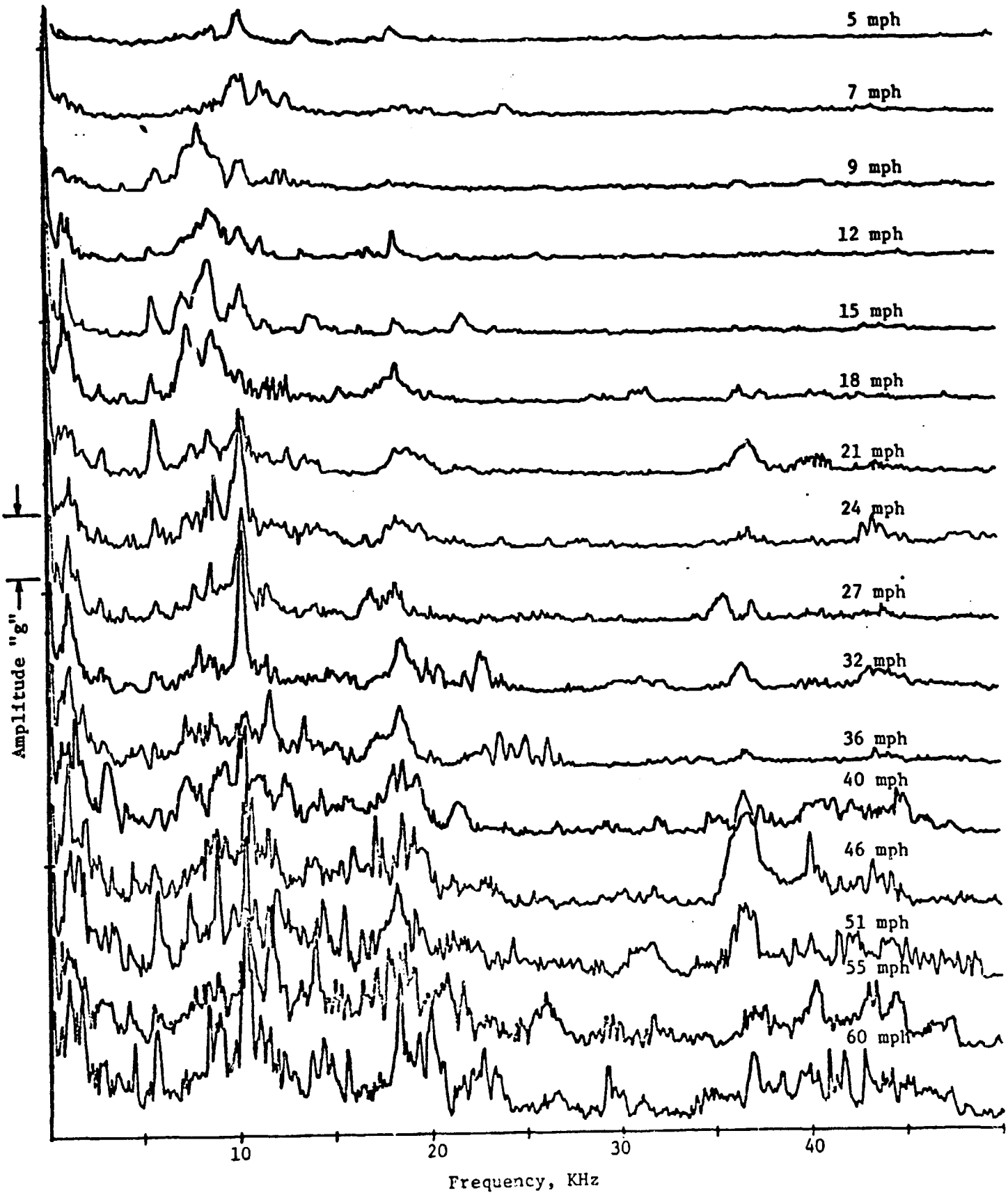

Fig. 18 New Bearing; Bearing Frequency Characteristics During Shutdown (New Bearing)

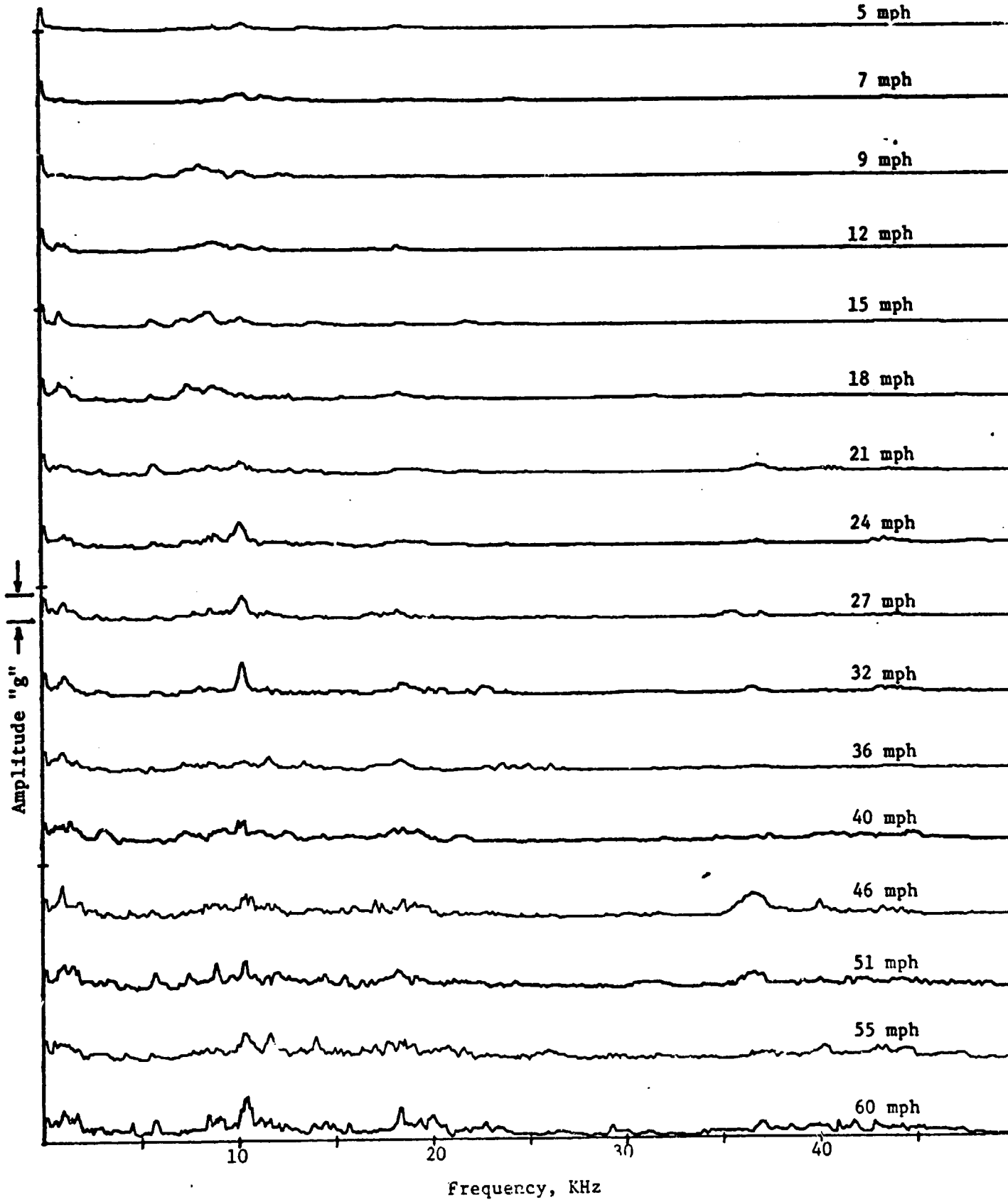

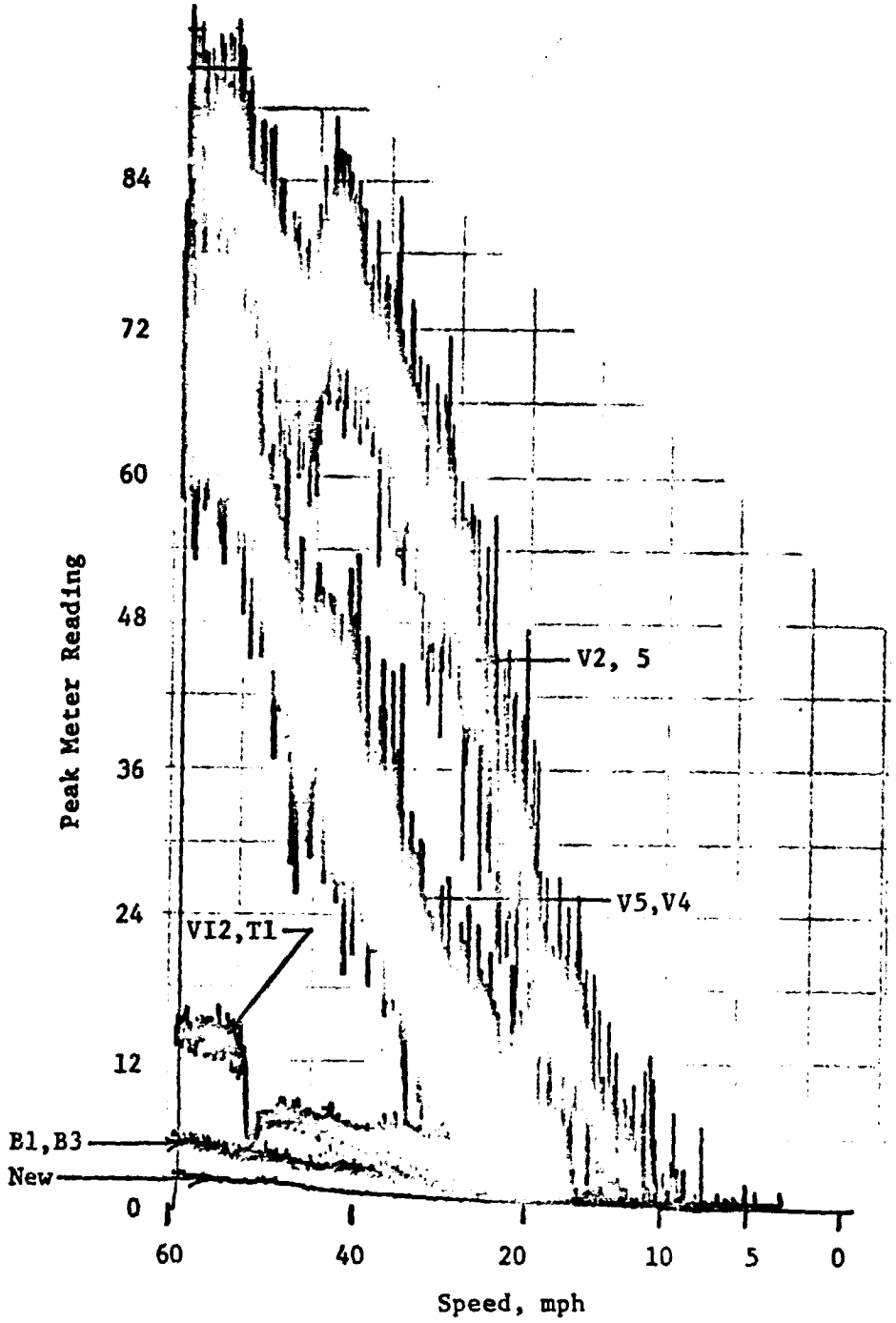


Fig. 19 Amplitude at 17 KHZ Versus Speed

"g is directional but the load orientation relative to the crack was not known during the test.

It is noted that a large variation in amplitude is recorded during coast-down for the damaged bearings. The amplitude variation is due to the modulation of the 17 KHz center frequency. Demodulation and a frequency analysis of bearing VI-2, T-1 and a new bearing is shown on Figure 20. The roller pass frequency at approximately 100 Hz and its third and fourth harmonic are evident. The new bearing shows no evidence of these frequencies and only running frequency is apparent.

Sound measurements were recorded on each bearing in the test rig with the microphone located six inches from the bearing. Analysis of the sound was conducted using a 10 KHz band pass filter. Frequency spectra of the sound is illustrated on Figure 21. The three sets of bad bearings had overall levels ranging from 3 to 13 db higher than the new bearings. Although a number of high frequencies in the 10 to 20 KHz range are evident, no discrete frequency with bearing modulating components were found consistently for each bearing as noted with acceleration. Sound, therefore, did not appear as suitable as structure borne vibration as a means of detecting faulty bearings.

Results of the truck dragging tests were not as successful as the grease rig tests. Figure 22 illustrates the amplitude level of the 10 KHz and 17 KHz band pass frequency as the truck with instruments mounted on it passes down the track. As evidenced, the amplitudes of the new bearings are higher than damaged bearings and provide no indication of a good or bad bearing. These results are not too surprising since the grease testing indicated that the discrete frequencies are lost in noise below 5 mph. If detection of a faulty bearing could not be discerned on the truck at low speed, there was no chance of picking up the fault through the track. To determine the suitability of the track as a transmitter of bearing faults would necessitate repeating the tests with truck speeds above 50 mph.

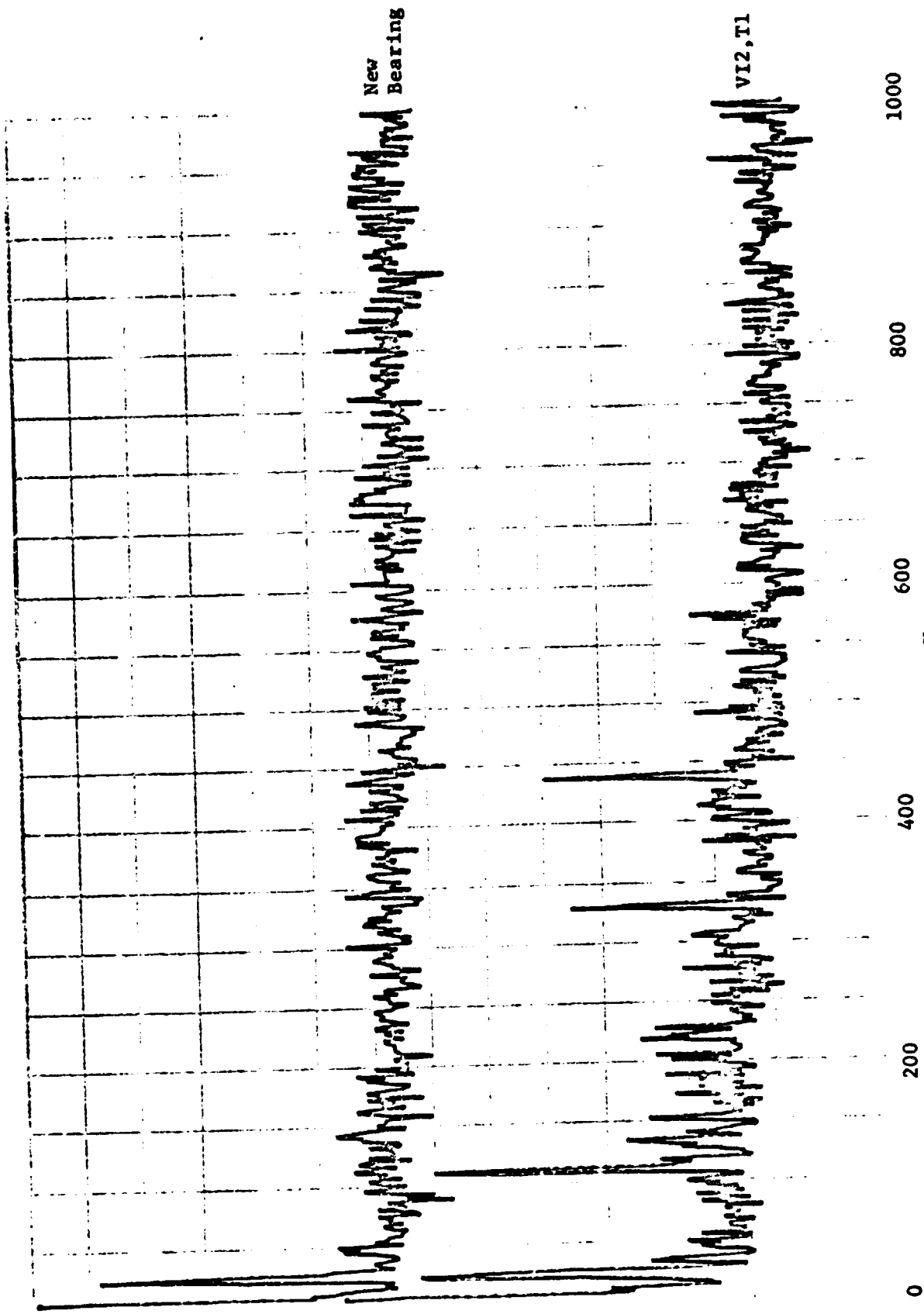


Fig. 20 Demodulation of 17 KHz Center Frequency

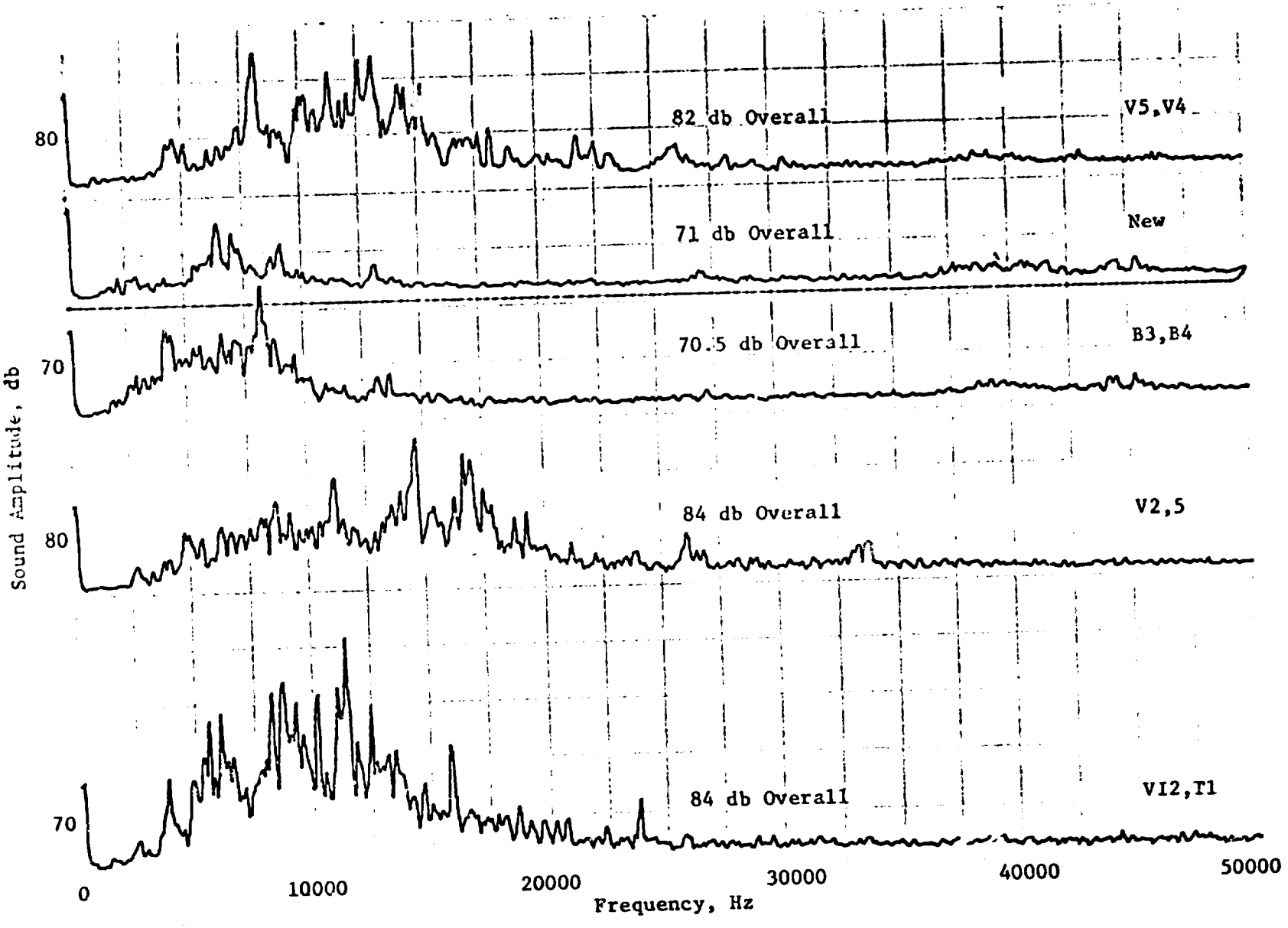


Fig. 21 Sound Frequency Spectra, Grease Test Rig at 60 mph

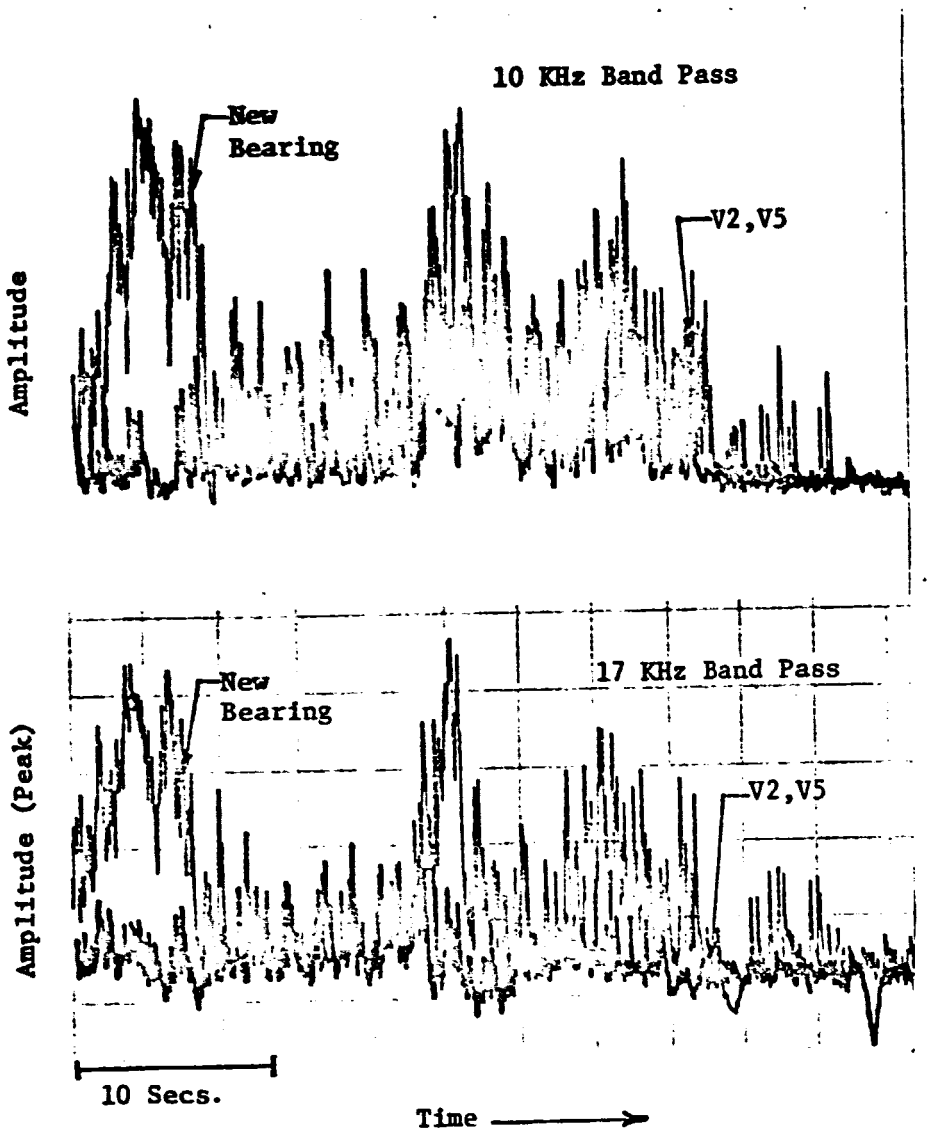


Fig. 22 Truck Dragging Tests

## SUMMARY

Laboratory tests on fifty seven bearings ranging from new to various degrees of damage indicated that structure-borne vibration in the 14 KHz to 20 KHz and 20 KHz to 30 KHz ranges could be used to discriminate between new and damaged bearings. Airborne sound in the same frequency ranges could also be utilized to categorize bearings but did not prove as discriminating as structure-borne acceleration. Demodulation of both 16 KHz and 22 KHz center frequencies permitted analysis of discrete bearing running frequencies for identification of the fault. The primary frequency observed was roller pass frequency.

A fault detector box breadboard was assembled to permit band pass filtering and demodulation of the frequencies of interest. The box was used for field testing of fully-assembled grease packed bearings.

Field testing of several damaged and new bearings were conducted on a grease test machine located at the AAR in Chicago. Acceleration and sound were recorded on the rig that accepted a complete axle assembly over an equivalent train speed range of 60 mph to standstill. High amplitude vibration was observed from the acceleration level in the 10 KHz and 17 KHz ranges. These frequencies were found to be driven to the high amplitudes by roller pass frequencies of damaged bearings. Below speeds of 25 mph, discrimination between good bearings and damaged bearings was difficult. With axles assembled on a truck and pushed at speeds below 5 mph, discrimination of damaged bearings could not be made.

The field tests on the grease test machine basically confirmed the data obtained in laboratory tests. The suitable ranges for detecting bearing damage differed in the field tests from 10 KHz and 17 KHz compared to 16 KHz and 22 KHz in the laboratory. However, the trends of amplitude followed the laboratory tests for good versus bad bearing.

## CONCLUSIONS AND RECOMMENDATIONS

The following conclusions were drawn based on program results:

1. The concept of utilizing high-frequency and modulation characteristics to identify damage in railroad roller bearings is a valid one.

2. High-frequency characteristics in the 16 KHz to 17 KHz range could be used to identify bearing faults in oil-lubricated bearings in the laboratory as well as on fully-assembled grease-packed bearings installed on axles.

3. High-frequency structure-borne vibration was more suitable than high-frequency airborne noise in identifying faulty bearings; however, sound levels for damaged bearings were 10 db higher than good bearings.

4. Bearing speeds greater than the equivalent of 25 mph are required to adequately separate good bearings from faulty bearings when the bearings are not loaded. Field data on heavily-loaded bearings were not obtained; however, it is expected that this should reduce the test speed.

5. Inspection of bearings at a derailment site is feasible utilizing a portable drive rig to operate the unloaded bearings at approximately 30 mph.

6. Although airborne noise results were promising, the feasibility of a wayside detection system utilizing either track mounted accelerometers or airborne noise cannot be assessed on the available data.

### Recommendations

The following recommendations are made to further implement the high-frequency technique as a means of detecting bearing faults after a car derailment without wheel disassembly:

1. Assemble a fault detector box with a fixed 17 KHz band

pass filter and adjustable amplitude level warning lights.

2. Assemble a portable axle drive rig which can be used to assemble damaged and new bearings and adjust amplitude levels on the fault detector box.

3. Ship the detector box and wheel test bed to a railroad rework shop for evaluation of bearings assembled on axles prior to teardown.

4. Conduct additional airborne noise tests with heated bearings.

## REFERENCES

1. Broderick, J.J., Burchill, R.F., and Clark, H.L., "Design and Fabrication of Prototype System for Early Warning of Impending Bearing Faults," Prepared Under Contract NAS8-25706 for NASA-MSFC by MTI, Latham, New York.

2. Burchill, R.F., "Resonant Structure Techniques for Bearing Fault Analysis," Paper Presented at 18th Meeting of the Mechanical Failures Group, Gaithersburg, Maryland, November 1972.